

## Short-range order effects on the electronic properties of a binary linear chain

Jaime Rössler and Gaston Martinez

*Facultad de Ciencias, Universidad de Chile, Casilla 653, Santiago, Chile*

Miguel Kiwi

*Departamento de Fisica, Universidad Simon Bolivar, Apartado 80659 Caracas 108, Venezuela*

(Received 26 September 1979)

A new technique to treat one-dimensional binary alloys, described in tight-binding approximation, capable of incorporating short-range correlations in a simple way is presented. The method is an extension of work by Faulkner and Korrington and handles spatial correlations by restricting the number of allowed configurations in the ensemble over which averages are taken. The density of electron states thus calculated exhibits rich structure, which is known to exist but is lost in treatments which neglect local correlation effects. A detailed study of the stoichiometric case with an equal number of atoms of both chemical species is presented, including up to next-nearest-neighbor correlations.

### I. INTRODUCTION

During the last decade the theory of disordered systems has received a great deal of attention; in particular, the electronic properties of binary alloys have been studied in great detail. However, most of the effort has been devoted to mean-field or coherent-potential-approximation (CPA) treatments of the fully random (or completely disordered) case, with the consequent smooth curves of the density of electron states, in spite of the facts that (a) detailed peak structures of the vibrational spectra, which are governed by equations formally analogous to the electronic spectra, are known to exist and to be related to local environment effects<sup>1</sup>; and (b) a good number of experiments indicate that short-range order determines some relevant electronic and magnetic behavior of alloys<sup>2</sup>.

A number of authors have included environmental disorder with varying degrees of success, as Falicov and Yndurain have pointed out<sup>3</sup>; most of these contributions take the CPA as their starting point.<sup>4</sup> Schwartz<sup>5</sup> provided a detailed comparison of different approaches and obtained expressions for some of the moments of the density of states, including short-range correlations. Later on Peterson *et al.*<sup>6</sup> investigated short-range-order effects in a one-dimensional hard-rod liquid model.

Weissmann and Cohan,<sup>7-9</sup> and more recently Cyrot-Lackmann and Cyrot,<sup>10</sup> have tackled the problem by solving exactly for a small cluster around an atom and then inserting it into an effective medium which is treated either in the virtual-crystal<sup>7-9</sup> or in the CPA<sup>10</sup> approximation. Falicov and Yndurain,<sup>3</sup> after diagonalizing the cluster of atoms, joined a Bethe lattice to each atom on the "surface" of it, this way enabling the treatment of both topological and substitutional disorder. Basis-

cally, the results of all these contributions<sup>3,7-10</sup> tend to underline the importance of short-range correlations, with the environment which surrounds the cluster playing only a minor role. In effect, no matter how this environment is treated the results that are obtained share the same essential features.

In this paper we use a completely different approach to study the electronic properties of a binary alloy; our method is an extension and generalization of the procedure due to the work of Faulkner and Korrington.<sup>11</sup> While restricted to the treatment of linear chains it has the following advantages:

- (a) it provides a real-space treatment, which incorporates short-range order in a very direct way;
- (b) it requires only an averaging process over the ensemble of allowed spatial configurations of the atoms which constitute the system, without invoking "effective potentials" or "effective media"; and
- (c) a whole wealth of spatial correlations such as nearest-neighbor, next-nearest-neighbor, . . . , short-range order parameters is introduced and handled in a very natural fashion.

We do consider a binary linear chain of *A*- and *B*-type atoms, with concentrations  $x_A$  and  $x_B$ , respectively, subject to the normalization  $x_A + x_B = 1$ . In addition, we characterize our results by the short-range-order parameter  $\lambda$  introduced in Ref. 3, which provides a nice tool for switching continuously from the perfectly ordered binary compound ( $\lambda = -1$ ), through the completely random configuration ( $\lambda = 0$ ), to the fully segregated structure ( $\lambda = 1$ ). Moreover, we also study effects related to higher correlations; while in this paper we only compute and discuss in some detail up to next-nearest-neighbor correlations, our method as developed below is well suited to be used beyond this limitation.

The rest of this paper is organized as follows: In Sec. II we analytically formulate our linear-chain tight-binding model of a binary alloy with no off-diagonal disorder, write down the Green's function difference equations, and solve them formally using the local transfer-matrix approach for a specific spatial configuration of atoms. The averaging process over different ensembles of allowed configurations is discussed next at length, at which point the crucial short-range-order correlations are introduced as constraints which determine the number of elements allowed in each specific ensemble. Finally, ensemble averages are evaluated using steepest descent techniques, which leads to self-consistency equations that have to be solved numerically. In Sec. III results of the numerical computation are presented and discussed, emphasizing and contrasting the role of nearest-neighbor and next-nearest-neighbor correlations, but limiting our attention at this time to the stoichiometric case  $x_A = x_B = 0.5$ . In Sec. IV the important physical consequences are stressed and some concluding remarks are made; a slight modification and adaptation to electron states of work carried out by Wu *et al.*<sup>12</sup> originally intended for treatment of vibrational spectra, is presented as an appendix, since it is used in Sec. III with the purpose of comparison with our results.

## II. MODEL AND FORMAL SOLUTION

### A. Single configuration case

As our model we choose a one-dimensional alloy with diagonal disorder as specified by the following tight-binding Hamiltonian:

$$H = \sum_j |j\rangle V_j \langle j| + T \sum_j (|j\rangle \langle j+1| + |j+1\rangle \langle j|), \quad (2.1)$$

where  $|j\rangle$  is a Wannier state associated with the  $j$ th lattice site,  $V_j = V_A, V_B$  are the energy levels of atoms  $A$  and  $B$ , respectively, and  $T$  is the hopping matrix element between nearest neighbors along the chain. We now define the "Greenian" or "resolvent" operator  $\hat{G}$  through

$$(E - H)\hat{G} = 1, \quad (2.2)$$

and take matrix elements between Wannier states to obtain

$$EG_{i,j} - V_i G_{i,j} - T(G_{i+1,j} + G_{i-1,j}) = \delta_{i,j}. \quad (2.3)$$

The usual approach is to solve this difference equation using continued fractions or closely related methods;<sup>7-10,12</sup> however, in this contribution a matrix approach is employed, which is possible since Eq. (2.3) can be set in the form

$$\begin{pmatrix} t_j & -1 \\ 1 & 0 \end{pmatrix} \begin{pmatrix} G_{j,0} \\ G_{j-1,0} \end{pmatrix} = \begin{pmatrix} 1/T \\ 0 \end{pmatrix} \delta_{j,0} + \begin{pmatrix} G_{j+1,0} \\ G_{j,0} \end{pmatrix}, \quad (2.4)$$

where  $t_j \equiv (E - V_j)/T$  and  $N \geq j \geq 0$ , with  $N$  being the total number of atoms in the linear chain. Equation (2.4) can be used iteratively; in order that this iteration process be closed we impose cyclic boundary conditions:  $G_{0,0} = G_{N,0}$ . Thus Eq. (2.3) implies that

$$t_0 G_0 = 1/T + G_{N-1} + G_1, \quad (2.5)$$

where we have chosen the notation  $G_{j,0} \equiv G_j$ , which we will use from now on for simplicity. At this point the local transfer matrix  $\underline{M}_j$  is defined as

$$\underline{M}_j \equiv \begin{pmatrix} t_j & -1 \\ 1 & 0 \end{pmatrix}. \quad (2.6)$$

Applying it repeatedly on  $\begin{pmatrix} G_N \\ G_{N-1} \end{pmatrix}$  we obtain

$$\begin{pmatrix} G_N \\ G_{N-1} \end{pmatrix} = \underline{M}_{N-1} \underline{M}_{N-2} \cdots \underline{M}_2 \underline{M}_1 \begin{pmatrix} G_1 \\ G_0 \end{pmatrix}, \quad (2.7)$$

but knowing from Eq. (2.5) that

$$\begin{pmatrix} t_0 & -1 \\ 1 & 0 \end{pmatrix} \begin{pmatrix} G_0 \\ G_{N-1} \end{pmatrix} = \begin{pmatrix} 1/T + G_1 \\ G_0 \end{pmatrix}, \quad (2.8)$$

we have

$$\begin{pmatrix} G_0 \\ G_{N-1} \end{pmatrix} = \underline{M} \begin{pmatrix} G_0 \\ 1/T + G_{N-1} \end{pmatrix}, \quad (2.9)$$

where  $\underline{M} = \prod_j \underline{M}_j$ .

The latter equation defines the  $2 \times 2$  total transfer matrix  $\underline{M}$  and allows us to write the propagator  $G_0$  in terms of the four components of  $\underline{M}$ , which we denote by  $m_{rs}$ , to obtain

$$G_0 = \frac{m_{12}}{1 - (m_{11} + m_{22}) + m_{11}m_{22} - m_{12}m_{21}} \frac{1}{T}. \quad (2.10)$$

Since  $m_{11} + m_{22} = \text{Tr} \underline{M}$  and  $m_{11}m_{22} - m_{12}m_{21} = \det \underline{M} = 1$  [from Eq. (1.6)], our final relation for the Green's function reads

$$G_0 = \frac{m_{12}}{\text{Tr}(\underline{1} - \underline{M})} \frac{1}{T}. \quad (2.11)$$

The transfer-matrix  $\underline{M}$  depends on the specific atomic configuration, which we denote by  $\alpha$ , and is a function of  $E$ ; the poles of  $G_0$  thus imply the following equation for the energy eigenvalues:

$$\text{Tr} \underline{M}(E, \alpha) = 2. \quad (2.12)$$

This relation is satisfied by  $N$  eigenvalues  $E_\mu$  and consequently

$$\text{Tr}[\underline{1} - \underline{M}(E, \alpha)] = - \prod_{\mu=1}^N \frac{E - E_{\mu}}{T}, \quad (2.13)$$

where the factor  $T^{-N}$  has been introduced for consistency with Eq. (2.6). Thus

$$\text{Tr} \underline{G}(E, \alpha) = \sum_{\mu=1}^N (E - E_{\mu})^{-1} \quad (2.14)$$

and we obtain for the integrated density of states  $N(E)$  the expression

$$N(E) = \int_{-\infty}^E dE' D(E') = \frac{-1}{\pi N} \text{Im} \ln \{ \text{Tr} [\underline{M}(E + i0^+, \alpha) - \underline{1}] \}, \quad (2.15)$$

where  $D(E)$  denotes the density of states per atom. It should be remarked that while the trace in Eq. (2.13) is taken over a  $2 \times 2$  matrix, the trace in (2.14) is taken over the  $N \times N$  matrix of the full Green's function  $G(E, \alpha)$  in the Wannier representation.

It is also interesting to note that the real part of the right-hand side of Eq. (2.15) can be interpreted as the inverse coherence length of an eigenstate of energy  $E$ , which we will denote by  $K(E)$ ; it represents the average pseudomomentum uncertainty of an eigenstate  $E$ . On the other hand, we know that  $k(E) \equiv \pi N(E)/a$  represents the average pseudomomentum associated with the energy eigenstate  $E$  and thus, we can rewrite the right-hand side of Eq. (2.15) as

$$\text{Re} \exp[ik(E) + K(E)] Na = \text{Tr} [\underline{M}(E, \alpha) - \underline{1}], \quad (2.16)$$

where the reasons for the positive sign of  $K(E)$  have been given by Faulkner and Korringa.<sup>11</sup>

### B. Average over configurations

Up to this point we have considered only *one* configuration of the many that the two kinds of atoms which make up our alloy can possess. From now on we will consider an *ensemble* of configurations  $\Xi$  with  $\Omega$  elements, each one of them occurring with the same probability. Thus the average density of states per atom is related to

$$\begin{aligned} \text{Tr} \underline{G}(E) &= \frac{1}{\Omega} \sum_{\alpha \in \Xi} \text{Tr} \underline{G}(E, \alpha) \\ &= \frac{\partial}{\partial E} \ln \prod_{\alpha=1}^{\Omega} \{ \text{Tr} [\underline{M}(E, \alpha) - \underline{1}] \}^{1/\Omega}, \end{aligned} \quad (2.17)$$

which is an exact result. The approximation of Faulkner and Korringa<sup>11</sup> is equivalent to taking an arithmetic average, instead of the geometric one of Eq. (2.17), which reads

$$\text{Tr} \underline{G}(E) \cong \frac{\partial}{\partial E} \ln \left( \frac{1}{\Omega} \sum_{\alpha=1}^{\Omega} \text{Tr} [\underline{M}(E, \alpha) - \underline{1}] \right). \quad (2.18)$$

Faulkner<sup>13</sup> and Ramírez and Rössler<sup>14</sup> have already pointed out that this approximation leads to results identical to those of the CPA.

The main purpose of the present contribution is to study effects due to short-range order, i.e., effects related directly to local deviations from the average of the probability of finding one of the chemical species. We incorporate these correlations by fixing the number of segments of pure A- or B-type atoms of a determined length; this way the number of allowed configurations in the ensemble  $\Xi$  is rather drastically reduced. Analytically

$$\Xi \equiv \Xi(L; N_A, N_B; P_1, P_2, \dots, P_r; Q_1, Q_2, \dots, Q_s), \quad (2.19)$$

where the ensemble  $\Xi$  contains all possible configurations of  $N_{A(B)}$  atoms of species A (B) with  $L$  disjoint segments of A atoms separating another set of  $L$  disjoint segments of B atoms. Of these segments  $P_1$  are one A atom long,  $P_2$  are two A atoms long, and  $P_j$  are A atom segments of length  $j$ ; the same holds true for B atoms, of which there are  $Q_j$  segments present of length  $j$ .

An enormous wealth of correlations in the spatial distribution is in this way introduced, well beyond what can be found in the existing literature. In fact, just by fixing the ratio  $L/N_A$  the nearest-neighbor correlation parameter  $\lambda_A$  of Falicov and Yndurain<sup>3</sup> becomes fully determined; since the probability of finding an AB pair is  $L/N_A$  (i.e., each of the  $L$  segments ends or starts with AB pair), it follows that  $\lambda_A = 1 - 2L/N_A$ .

In this paper we will basically restrict ourselves to fixing  $P_1$  and  $Q_1$  *in addition* to  $\lambda$ . In this way the number of binary and ternary segments also becomes determined; in effect, the probabilities of finding a specified ordered pair next (to the right or left) of an A atom, are given by

$$p_{A,AA} = \frac{N_A + P_1 - 2L}{N_A}, \quad (2.20a)$$

$$p_{A,AB} = \frac{L - P_1}{N_A}, \quad (2.20b)$$

$$p_{A,BA} = \frac{Q_1}{N_A}, \quad (2.20c)$$

$$p_{A,BB} = \frac{L - Q_1}{N_A}. \quad (2.20d)$$

Certainly, the normalization condition  $p_{A,AA} + p_{A,AB} + p_{A,BA} + p_{A,BB} = 1$  is satisfied; moreover, the binary correlation parameters are readily determined by summation over the last index.

Having defined our short-range correlation parameters we proceed to the averaging process proper; for convenience we denote as  $\underline{M}_A$  and  $\underline{M}_B$  the transfer matrices associated with sites A and

$B$ , respectively, and define the matrix function

$$\underline{F}(z_A, z_B, \xi, \eta) \equiv \left[ \left( \underline{M}_A z_A \xi + \sum_{j=2}^{\infty} \underline{M}_A^j z_A^j \right) \times \left( \underline{M}_B z_B \eta + \sum_{j=2}^{\infty} \underline{M}_B^j z_B^j \right) \right]^L. \quad (2.21)$$

Then, using an extended version of a method due to the work of Faulkner,<sup>15</sup> we obtain the average of the total transfer matrix  $\underline{M}$  over the ensemble  $\Xi$  as a contour integral which encloses the origin and which has the form

$$\langle \underline{M} \rangle = \frac{1}{\Omega} \frac{1}{(2\pi i)^4} \oint \oint \oint \oint \frac{dz_A dz_B d\xi d\eta}{z_A^{N_A+1} z_B^{N_B+1} \xi^{P_1+1} \eta^{Q_1+1}} \times \underline{F}(z_A, z_B, \xi, \eta). \quad (2.22)$$

The number of elements in the restricted ensemble  $\Omega$  is given by the expression

$$\Omega = \binom{L}{P_1} \binom{L}{Q_1} \binom{N_A - L - 1}{N_A + P_1 - 2L} \binom{N_B - L - 1}{N_B + Q_1 - 2L}. \quad (2.23)$$

Using the relation

$$(\underline{M}_A^{-1} - z_A)^{-1} = (\underline{M}_A - z_A) / [1 + z_A(z_A - t_A)],$$

where  $t_A$  was defined after Eq. (2.4), we can carry out the matrix summation in (2.21) to obtain

$$\underline{F}(z_A, z_B, \xi, \eta) = \left[ \frac{z_A^2}{\xi_A [1 + z_A(z_A - t_A)]} \frac{z_B^2}{\xi_B [1 + z_B(z_B - t_B)]} (\underline{M}_A - \xi_A)(\underline{M}_B - \xi_B) \right]^L, \quad (2.24)$$

where

$$\xi_A \equiv \frac{z_A}{(z_A - t_A)z_A(\xi - 1) + \xi},$$

$$\xi_B \equiv \frac{z_B}{(z_B - t_B)z_B(\eta - 1) + \eta}.$$

Diagonalization of the matrix  $(\underline{M}_A - \xi_A)(\underline{M}_B - \xi_B)$  of Eq. (2.24) yields the eigenvalues  $\Lambda_{\pm}$ ; they are

$$\Lambda_{\pm}(\xi_A, \xi_B) = \frac{1}{2} [t_A - \xi_A](t_B - \xi_B) + \xi_A \xi_B - 2] \pm \left[ \frac{1}{4} (t_A t_B - \xi_A t_B - \xi_B t_A)^2 - (\xi_A + \xi_B - t_A)(\xi_A + \xi_B - t_B) \right]^{1/2} \quad (2.25)$$

and thus

$$\langle \text{Tr} \underline{M} \rangle = \frac{1}{\Omega} \frac{1}{(2\pi i)^4} \oint \oint \oint \oint \frac{dz_A dz_B d\xi d\eta}{\xi^{P_1+1} \eta^{Q_1+1}} \frac{[\Lambda_+(\xi_A, \xi_B)]^L + [\Lambda_-(\xi_A, \xi_B)]^L}{z_A^{N_A-2L+1} z_B^{N_B-2L+1} \xi_A^L \xi_B^L [1 + z_A(z_A - t_A)]^L [1 + z_B(z_B - t_B)]^L}. \quad (2.26)$$

If we set  $\eta = \xi = 1$  in the equation above we recover the case treated by Falicov and Ynduráin, who kept only first-neighbor correlations (i.e., the parameter  $\lambda_A = 1 - 2L/N_A$  is fixed, but neither  $P_1$  nor  $Q_1$  are).

In Eq. (2.26) it is convenient to make the change of variables  $\{\xi, \eta\} \rightarrow \{\xi_A, \xi_B\}$ , to obtain

$$\langle \text{Tr} \underline{M} \rangle = \frac{1}{\Omega} \frac{1}{(2\pi i)^4} \oint \oint \oint \oint \frac{dz_A dz_B d\xi_A d\xi_B}{z_A^{N_A+P_1-2L+1} z_B^{N_B+Q_1-2L+1}} \frac{\Lambda_+^L + \Lambda_-^L}{\xi_A^{L-P_1+1} \xi_B^{L-Q_1+1} [1 + \xi_A(z_A - t_A)]^{P_1+1} [1 + \xi_B(z_B - t_B)]^{Q_1+1}} \times \frac{1}{[1 + z_A(z_A - t_A)]^{L-P_1} [1 + z_B(z_B - t_B)]^{L-Q_1}}, \quad (2.27)$$

which in turn can be written as

$$\langle \text{Tr} \underline{M} \rangle = \frac{1}{\Omega} \frac{1}{(2\pi i)^4} \oint \oint \oint \oint dz_A dz_B d\xi_A d\xi_B (e^{L\phi_+(z_A, z_B, \xi_A, \xi_B)} + e^{L\phi_-(z_A, z_B, \xi_A, \xi_B)}), \quad (2.28)$$

where

$$\phi_{\pm}(z_A, z_B, \xi_A, \xi_B) \equiv \ln \Lambda_{\pm}(\xi_A, \xi_B) - \frac{P_1}{L} \ln [1 + \xi_A(z_A - t_A)] - \frac{Q_1}{L} \ln [1 + \xi_B(z_B - t_B)] - \frac{N_A + P_1 - 2L}{L} \ln z_A - \frac{N_B + Q_1 - 2L}{L} \ln z_B - \frac{L - P_1}{L} \ln [\xi_A [1 + z_A(z_A - t_A)]] - \frac{L - Q_1}{L} \ln [\xi_B [1 + z_B(z_B - t_B)]] . \quad (2.29)$$

When Eqs. (2.16) and (2.28) are compared it is observed that the real and imaginary parts of the  $\phi_{\pm}$  functions are proportional to the inverse coherence length  $K(E)$  and the average pseudomomentum  $k(E)$ , respectively, when  $\phi_{\pm}$  are evaluated at the saddle points. The fact that this can safely be done is due to the large values that  $\exp(L\phi_{\pm})$  does assume. In order to find the extrema of  $\phi_{\pm}$  we set

$$\frac{\partial \phi_{\pm}}{\partial z_B} = 0, \quad (2.30a)$$

$$\frac{\partial \phi_{\pm}}{\partial z_A} = 0, \quad (2.30b)$$

from which  $\zeta_A = \zeta_A(z_A)$  and  $\zeta_B = \zeta_B(z_B)$  are obtained analytically. These expressions for  $\zeta_A$  and  $\zeta_B$  next are substituted in the additional equations for the extrema of  $\phi_{\pm}$ ,

$$\frac{\partial \phi_{\pm}}{\partial \zeta_A} = 0, \quad (2.31a)$$

$$\frac{\partial \phi_{\pm}}{\partial \zeta_B} = 0, \quad (2.31b)$$

which have to be solved numerically, thus completing the evaluation of  $\langle \text{Tr} M \rangle$ . Knowing this average, the density of states and the coherence length are readily obtained using Eqs. (2.18) and (2.16), respectively.

### III. RESULTS

We now present the results of the implementation on a computer of the scheme outlined in the preceding section. In order to display most clearly the important physical consequences of short-range correlations we have chosen to limit our interest, for the time being, to a stoichiometric binary alloy with an equal number of *A* and *B* atoms, denoted by  $x_A = N_A/N = N_B/N = x_B = \frac{1}{2}$ .

For the parameters that characterize the electronic structure, which appear in the basic Hamiltonian (2.1), we have chosen the following values:

(i) The energy is scaled in units of the hopping matrix element, which we make equal to  $T = \frac{1}{4}$ ; this way the bandwidth for the electron states of the pure *A* and *B* chains are equal to one.

(ii) For the diagonal matrix elements we make  $V_A = 0.5$  and  $V_B = 0.15$ . This way the pure *A* and *B* bands extend from 0 to 1, and from -0.35 to 0.65, respectively.

In Fig. 1 we display results of the density of electron states  $D(E)$ , normalized to one state per atom, computed with our method when only the parameter  $\lambda_A$  of Ref. 3 is fixed; since  $\lambda_A = 1 - 2L/N_A$  we only fix the number of segments  $L$  in addition to the stoichiometry imposed above. In other words, we are not assigning values to the  $P_j$ 's and  $Q_j$ 's of Eq. (2.19) at this point. As  $\lambda$  increases from -1 to 1 (i.e., from a binary alloy to full segregation) several interesting features can be ob-

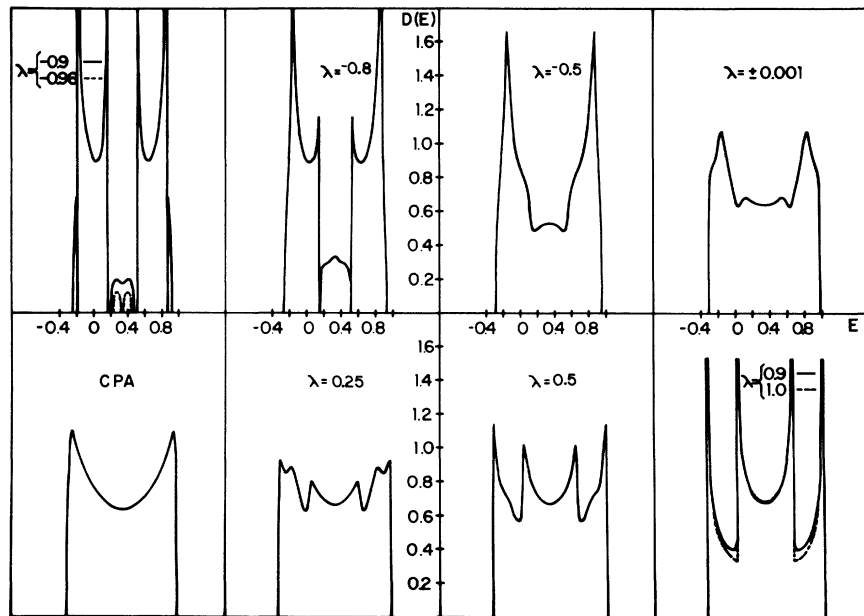


FIG. 1. Density of electron states  $D(E)$ , normalized to one state per atom, versus energy for values of the nearest-neighbor correlation parameter varying between  $-1 < \lambda \leq 1$ . The value  $\lambda = -1$  corresponds to a binary superstructure and  $\lambda = 1$  to full segregation;  $\lambda = 0$  describes an uncorrelated random alloy.

served:

(a) At first ( $\lambda = -0.96$  and  $-0.9$ ) the essential characteristics of the translationally invariant superstructure  $\cdots ABAB \cdots$  are dominant, however, split-off states corresponding to bonding and antibonding orbitals around  $AA$  and  $BB$  "defects" make their appearance in the gaps of the translationally invariant electronic structure.

(b) For  $\lambda = -0.8$  the gap between the two main sub-bands has practically disappeared, while the bottom and top of the band are still quite far apart from the "true band edges"<sup>16</sup> in the Lifshitz sense which are  $-0.35$  and  $1$ , respectively.

(c) As  $\lambda = -0.5$  the four-peak structure due to translational invariance has completely disappeared to give way to two sharp peaks and a smooth maximum at the center of the band.

(d) For  $\lambda = 0$  the random configuration is reached and it is quite apparent that our method retains a lot more "structure" in the electronic density of states than the CPA does, or equivalently,<sup>13,14</sup> than the one obtained through Eq. (2.12) and averaging over *all* possible configurations. This is due to the fact that our average is performed over a much smaller number of configurations, which, while yielding more detailed structure than the full ensemble of random configurations, has identically the same entropy; this point will be discussed in greater detail below.

(e) As  $\lambda$  continues increasing to  $0.25$  and  $0.5$  we observe the gradual appearance of the four-peak structure of the fully segregated configuration  $\lambda = 1$ ; the latter simply corresponds to the superposition of a pure  $A$  band, which extends from  $0$  to  $1$ , and a  $B$  band ranging from  $-0.35$  to  $0.65$ .

In Fig. 2 plots of the inverse coherence length  $K(E)$ , defined after Eq. (2.15), as a function of the energy  $E$  and for three values of  $\lambda$  are displayed, providing some complementary information on the nature of the electron states. As expected on the basis of qualitative arguments, the maximal co-

herence length occurs for  $\lambda \geq -1$  and  $\lambda \leq 1$ .

In fact, for  $\lambda = -0.9$  the bulk of the band is made up of  $ABAB \cdots$  superstructure eigenstates, while bonding and antibonding states with small spatial spread are present at both ends and at the center of the band. Analogously, for  $\lambda = 0.9$  the center of the band consists of extended states related to long  $A$ - or  $B$ -atom segments. Also as expected, electron states associated to the random  $\lambda = 0$  configurations exhibit significantly smaller spatial coherence. In addition it is interesting to note that in the forbidden energy regions (gaps) the plot of  $K(E)$  simply seems to be quenched, with no singular behavior associated with it.

In Fig. 3 we focus on the most relevant qualitative results in this contribution and compare with related work<sup>12</sup>; in effect, the density of states computed through the CPA (upper left) and an adaptation of Wu's method, which is detailed in the Appendix (lower right), are provided to contrast our own results.

The difference in approach to obtain the CPA and  $\lambda = \pm 0.001$  graphs is that in the first case Eq. (2.12) is solved averaging over

$$\Omega = \begin{bmatrix} N \\ N_A \end{bmatrix} = \begin{bmatrix} N \\ N/2 \end{bmatrix},$$

equally probable configurations (recall that  $N_A = N_B$  throughout), while in the latter we fix also the number  $L$  of pure  $A$  (or  $B$ ) atom segments. Thus, while in the CPA there is a total absence of correlations between atoms, for  $\lambda = \pm 0.001$  we impose the *additional* requirement of absence of short-range correlations; analytically, this implies that the probability  $p_A$  of finding an  $A$  atom next to another  $A$  atom is

$$p_A = x_A, \quad (3.1)$$

or in words: The presence of an atom at a given site does not influence the probability of finding

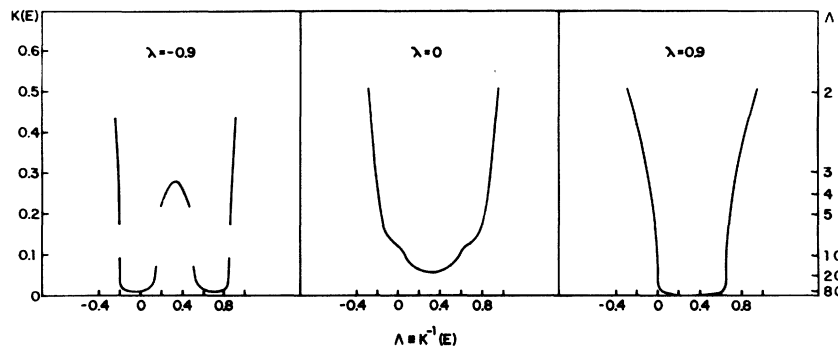


FIG. 2. Inverse coherence length  $K(E) = \Lambda^{-1}$  versus energy for alloys near the superstructure ( $\lambda = -0.9$ ), in the random ( $\lambda = 0$ ), and near the fully segregated ( $\lambda = 0.9$ ), configurations.

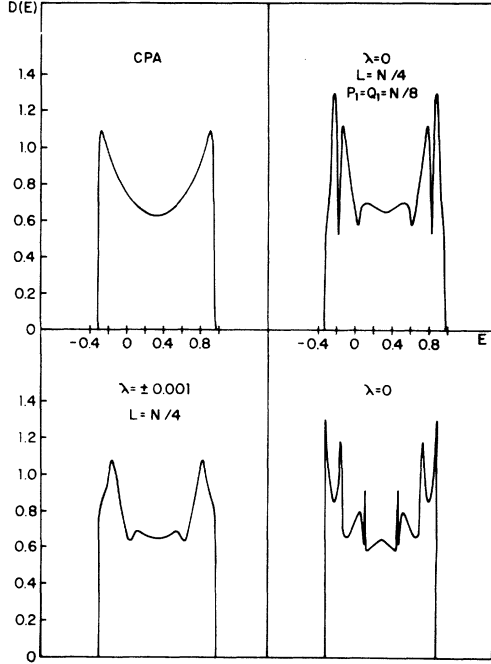


FIG. 3. Density of states  $D(E)$  versus energy. The upper left corresponds to coherent potential approximation results. The lower left and upper right are our results when no nearest-neighbor and no next-nearest-neighbor spatial correlation requirements are imposed, respectively. The lower right plot corresponds to a calculation carried out on the basis of a scheme due to the work of (Ref. 12).

A or B at the neighboring site. Since in general

$$1 - p_A = L/N_A, \quad (3.2)$$

we obtain  $L/N = \frac{1}{4}$  as the condition for no nearest-neighbor correlations. In this case the number of elements in the ensemble of configurations is reduced to

$$\Omega = \binom{N_A}{L} \times \binom{N_B}{L} = \binom{N/2}{N/4}^2,$$

which is significantly smaller than the value of  $\Omega$  used in connection with the CPA. However, since

$$\ln \binom{N}{N/2} \xrightarrow{N \rightarrow \infty} N \ln 2 \quad (3.3)$$

and also

$$2 \ln \binom{N/2}{N/4} \xrightarrow{N \rightarrow \infty} N \ln 2, \quad (3.4)$$

the entropy and thus all thermodynamic properties are identical for both cases. In consequence, taking averages over "smaller" ensembles has the effect of retaining structure in the density of states

which is "ironed" out in the conventional approaches like the CPA, while the correct thermodynamic properties are rigorously preserved.

To obtain the  $\lambda=0$  plot of the upper right in Fig. 3 we have restricted the ensemble even further by adding to the absence of first-neighbor correlations the requirement of no next-nearest-neighbor correlations. Analytically this condition is

$$p_{R,S,T} = p_{R,S} p_{S,T}, \quad (3.5)$$

where  $R, S, T = A, B$ .  $p_{R,S,T}$  was defined in connection with Eqs. (2.20) and  $p_{R,S} = p_A$  if  $R = S = A$  and  $p_{R,S} = 1 - p_A$  if  $R = A \neq S$ . Using Eqs. (2.20b) and (2.20c) in combination with (3.5) yields

$$P_1 = L^2/N_A, \quad (3.6)$$

$$Q_1 = L^2/N_B. \quad (3.7)$$

However, we had  $L/N = \frac{1}{4}$  and thus the requirement of no next-nearest-neighbor correlations is satisfied for

$$P_1 = Q_1 = \frac{1}{8}N.$$

This way, the ensemble associated with the plot characterized by  $\lambda=0$ ,  $L = \frac{1}{4}N$ , and  $P_1 = Q_1 = \frac{1}{8}N$  has

$$\begin{aligned} \Omega &= \binom{L}{P_1} \binom{L}{Q_1} \binom{N_A - L - 1}{L - P_1 - 1} \binom{N_B - L - 1}{L - Q_1 - 1} \\ &\cong \binom{N/4}{N/8}^4 \end{aligned}$$

different configurations; again, the limit as  $N \rightarrow \infty$  yields the same value for the entropy as obtained in Eqs. (3.3) and (3.4). However, when looking at the upper right of Fig. 3 important changes are observed in relation to the lower left plot; the four-peak structure has evolved into a six-peak spectrum. These six peaks are in good agreement in position as well as magnitude with the main peaks obtained using the method outlined in the Appendix, which is an extension of work by Wu.<sup>12</sup>

Finally, in Fig. 4 we display results with next-nearest-neighbor correlation, but require absence of correlation to first neighbors; this can be achieved by choosing  $L = \frac{1}{4}N$ , but  $P_1 \neq \frac{1}{8}N$ . In fact, the left-hand graph is for  $P_1 = 0.08N < 0.125N$ ; thus there is a deficit of single atom segments as compared with the uncorrelated situation. This way an excess of  $AABB \dots$ -type sequences builds up. On the other hand, when this four-atom sequence is infinitely repeated we are faced with a problem which can be solved exactly; we have done so and found that the peaks near the edges and the center of the band effectively correspond to the  $AABB \dots$  superstructure and that the maxima at  $E \approx 0.76$  and  $-0.11$  are related to "defects" in res-

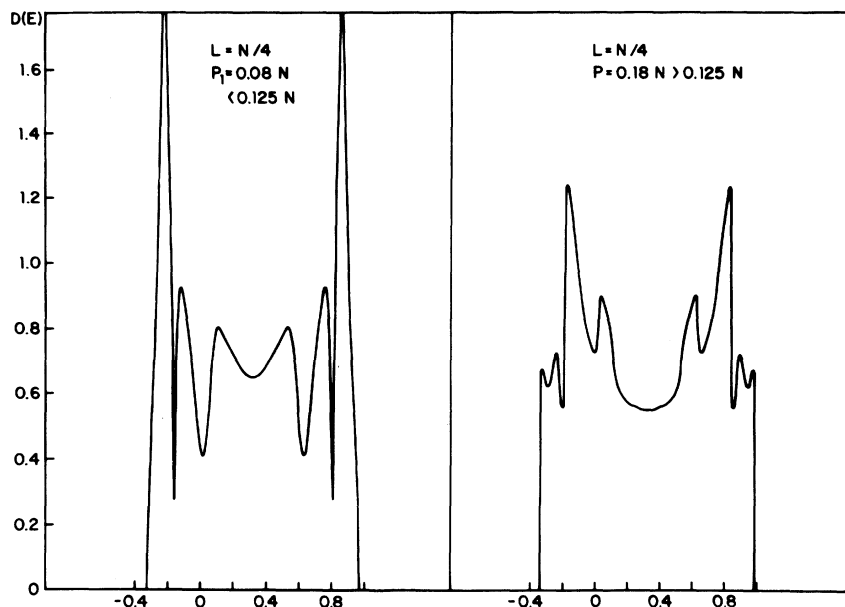


FIG. 4. Density of states versus energy with no nearest-neighbor correlation, but where next-nearest-neighbor correlation is imposed.  $P_1 = 0.08N$  corresponds to a deficit and  $P_1 = 0.18N$  to an excess of isolated  $A$  atoms, relative to the uncorrelated  $P_1 = 0.125N$  case.

pect to this sequence.

The right-hand plot of Fig. 4 corresponds to  $P_1 = 0.18N > 0.125N$  and therefore an excess of isolated  $A$  and  $B$  atoms is present. Since the total number  $L$  of segments is fixed, the remaining atoms tend to form long  $A$  and  $B$  chains; consequently the corresponding density of states consists of a superposition of characteristic elements of both the  $\lambda \geq -1$  (binary alloy) and  $\lambda \leq 1$  spectra displayed in Fig. 1.

#### IV. SUMMARY AND CONCLUSIONS

A technique to treat one-dimensional binary alloys including local-order effects has been presented. Basically, it consists in a generalization of the method due to Faulkner and Korringa,<sup>11,15</sup> in order to include short-range-order effects; this purpose is achieved by restricting the number of allowed spatial atomic configurations in the ensemble used to obtain the averages of the quantities of physical interest. After some algebraic manipulation these averages are expressed as multiple contour integrals in the complex plane and are evaluated using saddle-point integration, which in turn leads to a set of self-consistency equations.

If up to next-nearest-neighbor correlations are kept the complex contour integrals become four-fold. The resultant self-consistency equations can be reduced in part analytically, but a final set has to be handled numerically.

This scheme was carried out for the stoichio-

metric case of equal number of atoms of each of the two chemical species and it was found that the stronger the local correlation included in the calculations, the richer the structure of the computed electronic spectra. On the other hand, our results for the density of states compare quite well with those obtained through an adaptation of a procedure proposed by Wu.<sup>12</sup> Moreover, they are fully consistent with semiquantitative arguments based on exact evaluations of the spectra of several superstructures, generated by repeating periodically particular sequences or clusters of atoms, which serve to identify the position and origin of the main peaks in the alloy density of states. While we have limited our attention, for the time being, to the case of equal concentration of the two binary species it would be of interest to study some additional stoichiometric situations and also the consequences of deviations from stoichiometry around the binary compound limit ( $\lambda = -1$ ) or near the fully segregated situation ( $\lambda = 1$ ), which could have interesting physical consequences.

#### ACKNOWLEDGMENTS

One of us (M.K.) gratefully acknowledges the warm hospitality received at the Faculty of Sciences of the University of Chile while this work was carried out and the partial support of the Organization of American States (OAS). We thank Dr. Mariana Weissmann for carefully reading the manuscript and for stimulating comments and



acknowledge an enlightening discussion of our results with Professor L. M. Falicov.

#### APPENDIX

In this appendix we slightly modify work by Wu *et al.*,<sup>12</sup> in order to adapt it to handle short-range-order effects on the electronic structure of linear chains, rather than the vibrational properties for which it was designed and used up to now. We start by writing Eq. (2.3) in the form

$$A_i G_{i,j} = (1/T) \delta_{i,j} + G_{i-1,j} + G_{i+1,j}, \quad (\text{A1})$$

where  $A_i \equiv (E - V_i)/T$ . In particular, we have

$$A_0 G_0(E) = 1/T + G_{-1} + G_1, \quad (\text{A2a})$$

$$A_1 G_1(E) = G_0 + G_2, \quad (\text{A2b})$$

...

$$A_n G_n(E) = G_{n-1} + G_{n+1}. \quad (\text{A2c})$$

Substituting in the above equation the definition

$$B_n^\pm \equiv \frac{G_{\pm(n+1)}}{G_{\pm n}}, \quad (\text{A3})$$

we obtain

$$B_{n-1}^+ = \frac{1}{A_n - B_n^+}. \quad (\text{A4})$$

When this expression is iterated it yields

$$B_0^+ = \frac{1}{A_1 - \frac{1}{A_2 - B_2^+}} = \frac{1}{A_1 - \frac{1}{A_2 - \frac{1}{A_3 - \frac{1}{\vdots - \frac{1}{\vdots - \frac{1}{\vdots - \frac{1}{A_m - B_m^+}}}}}}}} \quad (\text{A5})$$

and similarly

$$B_0^- = \frac{1}{A_{-1} - \frac{1}{A_{-2} - \frac{1}{A_{-3} - \frac{1}{\vdots - \frac{1}{\vdots - \frac{1}{A_{-m} - B_{-m}^-}}}}}}}. \quad (\text{A6})$$

Combination of (A2a), (A5), and (A6) yields

$$TG_0 = \frac{1}{A_0 - \frac{1}{A_1 - \frac{1}{A_2 - \frac{1}{\vdots - \frac{1}{\vdots - \frac{1}{A_m - B_m^+}}}}} - \frac{1}{A_{-1} - \frac{1}{A_{-2} - \frac{1}{\vdots - \frac{1}{\vdots - \frac{1}{A_{-m} - B_{-m}^-}}}}}}}. \quad (\text{A7})$$

If we now assume to know the configuration of the  $(2m+1)$  atoms in the domain  $\{-m, m\}$ , then Eq. (A7) is exact; however, we do not know the values of  $B_m^\pm$  which are determined by the configuration the rest of the atoms are in, i.e., those outside  $\{-m, m\}$ , about which we lack precise information. To overcome this difficulty an average over all possibilities is performed incorporating nearest-neighbor correlations; more precisely, the exact equation

$$B_j = \frac{1}{A_{j+1} - \frac{1}{A_{j+2} - \frac{1}{\vdots - \frac{1}{\vdots - \frac{1}{A_{N/2} - B_{N/2}}}}}}}. \quad (\text{A8})$$

is approximated by

$$B_j \cong \sum_{\sigma(j+1), \dots, \sigma(3j)} P_{\sigma(j), \sigma(j+1)} P_{\sigma(j+1), \sigma(j+2)} \cdots P_{\sigma(3j-1), \sigma(3j)} \frac{1}{A_{\sigma(j+1)} - \frac{1}{A_{\sigma(j+2)} - \frac{1}{A_{\sigma(j+3)} - \frac{1}{\vdots - \frac{1}{\vdots - \frac{1}{A_{\sigma(3j)} - B_{\sigma(3j)}}}}}}}, \quad (\text{A9})$$

where  $\sigma(j) = A, B$  and  $p_{\sigma(k), \sigma(k+1)}$  gives the probability of finding an atom of species  $\sigma(k+1)$  when site  $k$  is

occupied by species  $\sigma(k)$ .

Equation (A9) represents a self-consistent set of two equations [ $\sigma(j) = A, B$ ] for two unknowns:  $B_A$  and  $B_B$ ; once these equations are solved, we substitute in Eq. (A7) the values of  $B_m^+ = B_{\sigma(m)}$  and  $B_m^- = B_{\sigma(-m)}$  to obtain an approximate expression for the propagator, valid for the specified configuration of the original  $(2m+1)$ -atom cluster. However, this propagator contains much more information than we really want; to obtain the density of states an average over the  $2^{(2m+1)}$  allowed configurations of the cluster is performed, to obtain

$$D(E) = \sum_{\sigma(-m), \dots, \sigma(m)} x_{\sigma(0)} \dot{p}_{\sigma(0), \sigma(1)} \dots \dot{p}_{\sigma(m-1), \sigma(m)} \dot{p}_{\sigma(0), \sigma(-1)} \dots \dot{p}_{\sigma(-m+1), \sigma(-m)} \times D(E; \sigma(-m), \dots, \sigma(0), \dots, \sigma(m)), \quad (\text{A10})$$

where  $x_{\sigma(0)} = x_A, x_B$  is the concentration of the chemical species and

$$D(E; \sigma(-m), \dots, \sigma(0), \dots, \sigma(m)) = \frac{1}{\pi T} \text{Im} \left| \frac{1}{A_{\sigma(0)} - \frac{1}{A_{\sigma(1)} - \frac{1}{A_{\sigma(-1)} - \frac{1}{A_{\sigma(m)} - B_{\sigma(m)}} - \frac{1}{A_{\sigma(-m)} - B_{\sigma(-m)}}}} \right|_{E-i0^+}. \quad (\text{A11})$$

<sup>1</sup>See for instance, J. Hori, *Spectral Properties of Disordered Chains and Lattices* (Pergamon, Oxford, 1968); R. J. Elliott, J. A. Krumhansl, and P. L. Leath, *Rev. Mod. Phys.* **46**, 465 (1974).

<sup>2</sup>See for instance, J. D. Perrier, B. Tissier, and R. F. Tournier, *Phys. Rev. Lett.* **24**, 313 (1970); B. Chornik, M. Kiwi, and M. J. Zuckermann, *J. Phys. F* **6**, 2419 (1976).

<sup>3</sup>L. M. Falicov and F. Ynduráin, *Phys. Rev. B* **12**, 5664 (1975).

<sup>4</sup>F. Brouers, M. Cyrot, and F. Cyrot-Lackmann, *Phys. Rev. B* **7**, 4370 (1973); H. Miwa, *Prog. Theor. Phys.* **52**, 1 (1974); W. H. Butler, *Phys. Rev. B* **8**, 4499 (1973).

<sup>5</sup>L. M. Schwartz, *Phys. Rev. B* **7**, 4425 (1973).

<sup>6</sup>H. K. Peterson, L. M. Schwartz, and W. H. Butler, *Phys. Rev. B* **11**, 3678 (1975).

<sup>7</sup>M. Weissmann and N. V. Cohan, *J. Phys. C* **8**, 109 (1975).

<sup>8</sup>M. Weissmann and N. V. Cohan, *J. Phys. C* **9**, 473 (1976).

<sup>9</sup>N. V. Cohan and M. Weissmann, *J. Phys. C* **10**, 383 (1977).

<sup>10</sup>F. Cyrot-Lackmann and M. Cyrot, *Solid State Commun.* **22**, 517 (1977).

<sup>11</sup>J. S. Faulkner, and J. Korrington, *Phys. Rev.* **122**, 390 (1961).

<sup>12</sup>S. Y. Wu, C. C. Tung, and M. Schwartz, *J. Math. Phys.* **15**, 938 (1974); S. Y. Wu, *ibid.* **15**, 947 (1974); *Phys. Status Solidi B* **69**, K95 (1975); J. A. Cocks and S. Y. Wu, *ibid.* **77**, K5 (1976).

<sup>13</sup>J. S. Faulkner, *Phys. Rev. B* **1**, 934 (1970).

<sup>14</sup>J. Rössler and R. Ramírez, *Phys. Lett. A* **53**, 278 (1975); *J. Phys. C* **9**, 3747 (1976).

<sup>15</sup>J. S. Faulkner, *Phys. Rev. A* **135**, 124 (1964).

<sup>16</sup>I. M. Lifshitz, *Usp. Fiz. Nauk* **83**, 617 (1964) [*Sov. Phys. Usp.* **7**, 549 (1965)].